

Key words: *turboprop and turboshaft engines, modifications*

STANISLAW ANTAS^{*)}

THE AERO-THERMODYNAMIC ASPECTS OF THE METHODS FOR DESIGN MODIFICATIONS OF TURBOPROP AND TURBOSHAFT ENGINES

This article presents shortly reasons for improving designs of turboprop and turboshaft engines, and describes aero-thermodynamic aspects of methods of modification of these devices. The theoretical analysis of methods of modification concerns general changes of efficiency, flow, and rating. The influence of the following factors on engine performance is presented: change of efficiency of engine units, increase of compression and flow rate by using a compressor zero-stage, change of compressor pressure ratio, changes of gas temperature keeping the gasgenerator rotational speed constant by adjusting the minimal throat area of turbine nozzle guide vanes, turbomachinery modelling, and changes of rotational speed of ratings.

Nomenclature

- A - mass flow parameter,
- c - absolute velocity,
- C_e - specific fuel consumption,
- F - section area,
- G - mass flow rate,
- k - isentropic constant,
- M - Mach number,
- n - rotational speed,
- N - power,
- p_i^* - stagnation pressure in a given control section,

^{*)} *Transport Equipment Enterprise, WSK „PZL-Rzeszów” S.A; ul. Hetmańska 120, 35-078 Rzeszów, Poland; E-mail: eantas@prz.rzeszow.pl,*

- T_i^* - stagnation temperature in a given control section,
 s_f - continuity equation constant for air,
 β - correction coefficient,
 π - compression ratio of compressor, or expansion ratio of turbine,
 σ - recovery factor of total pressure,
 η - efficiency,
 λ - Laval number,
 $q(\lambda)$ - mass flux density, $c\rho/c_{crit}\rho_{crit}$,
 ρ - density,
 μ - flow rate coefficient,
 Subscripts and superscripts:
 /* - stagnation,
 /' - gas,
 /IN - inlet,
 /C - compressor,
 /B - combustion chamber,
 /CT - compressor turbine,
 /PT - power turbine,
 /D - exhaust diffuser,
 /GV - nozzle vane,
 /A - axial,
 /R - radial,
 /crit - critical value,
 /cor - corrected,
 /dp - design point,
 /st - stage,
 /1,2,...6 - control sections.

1. Introduction

The practise of designing shows that the development of aircraft turbine engines may proceed in two directions: the first direction is connected with developing the so-called base engines that determine appearing of new generations of engines, while the second one includes modernization and modifications. The basic reason for developing base engines is to improve efficiency of aircraft or helicopter functioning by a step increase of engine power with simultaneous lowering of unit costs. In spite of huge costs of developing new generation engines (from a few hundred millions to a few billions of USD), the designs grow old. The requirement of preventing this process and maintaining a product to be competitive needs continuous improvement of the power unit.

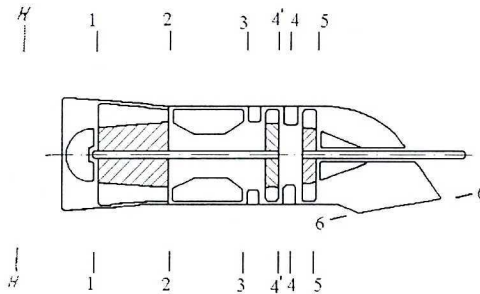


Fig. 1. Designations of control planes of a turboshaft and turboprop engine with free power turbine

The matter of improvement is practically resolved by making modifications on the ground of the base engine while maintaining maximal degree of part unification and by creating (approximately every 10 years) new types of base engines. The modification is a process of changing one or few base engine properties, including adaptation for performing new qualitative tasks, change of performance, improvement of manufacturing, and improvement of economical operation.

This proceeding makes it possible to decrease significantly time and costs of development and does not force step change of technology state, providing at the same time evolutionary progress in successive generations.

It should be emphasised that despite numerous examples of applying modifications of turboshaft and turboprop engines given in the literature [6], [7], [14], [16] only few theoretical works concern thermogasdynamical problems [12]. On the other hand, these problems are not fully described in the literature.

Obviously, possibilities of modification are limited, and when they are exhausted, it is necessary to develop next base engine.

2. Efficiency improvement

The output shaft power of a turboshaft engine with free power turbine and preliminary reducer at chosen flight conditions is determined by the relation:

$$N_{ePT} = G_{PT} \frac{k' R'}{k' - 1} T_4^* \left(1 - \frac{1}{\pi_{PT}^* \frac{k'}{k'}} \right) \eta_{PT}^* \eta_{mPT} \eta_R \quad (1)$$

where: R' – gas constant,

π_{PT}^* – total pressure ratio of combustion gas in a power turbine,

η_{mPT} – mechanical efficiency of gas producer shafting-line.

For a turboshaft engine with free power turbine without preliminary reducer $\eta_R = 1$. For both types of the engines, the working line of a compressor and compressor turbine assumes the form [4]:

$$\sqrt{\frac{\pi_C^*}{\eta_C^*}} = B q(\lambda_1) \sqrt{\frac{kR}{k-1} \frac{\beta}{k'R'} \left(1 - \frac{1}{\pi_{CT}^* \frac{k'-1}{k'}}\right) \eta_{mCT} \eta_{CT}^*} \quad (2)$$

where:

$$B = \frac{s_f}{s'_f} \frac{F_1}{(F_{GV})_{CT}} \frac{\mu_1}{q(\lambda_{GV})_{CT} \sigma_B \sigma_{GVCT} \mu_{GVCT}} \quad (3)$$

The equations presented shows that the changes of recovery factors of total pressure and efficiencies of assemblies directly influence engine performance, and, moreover, determine the costs of operation.

Table 1 presents the changes of shaft power value ($\Delta N_c = N_c - N_{c,dp}$) and specific fuel consumption ($\Delta C_c = C_c - C_{c,dp}$) of the aviation turboprop engine PZL-10S at assumed increase of recovery factors of total pressure and efficiency of assemblies $\Delta \eta_i = \Delta \sigma_i = 1\%$ (above design point values).

Table 1.

The influence of increase of recovery factors of total pressure and efficiencies of assemblies of the engine PZL-10S on the changes of power and specific fuel consumption

$$(\pi_{C,dp}^* = 7.4; T_{3,dp}^* = 1125 \text{ K, } S/L, \text{ static, ISA})$$

Performance change	Design point values							
	σ_{IN}	η_C^*	σ_B	η_B	η_{CT}^*	σ_{MT}	η_{PT}^*	σ_D
	0.985	0.79	0.95	0.97	0.88	0.98	0.89	0.96
ΔN_c [%]	+1.24	+2.4	+1.28	+0.07	+1.82	+1.25	+1.12	+1.27
ΔC_c [%]	-1.22	-1.8	-1.27	-1.02	-1.78	-1.26	-1.1	-1.26

The calculations were made using the OST program whose algorithm is presented in the paper [1]. The calculation results given in Table 1 show the tendency of power and specific fuel consumption change. They also give indications for choosing the modification direction purposed to change efficiency and recovery factor of total pressure for particular turboprop engine assemblies. Table 1 shows that the efficiencies of a compressor and turbines have a strong influence on engine performance, and that the efficiency of

another assemblies have a slightly weaker influence on it. The increase of efficiency of turbo-machines is due to geometry and losses optimisation at rims using computational fluid dynamics (trailing-edge thickness correction, Reynolds-number correction through enhancing surface texture, secondary-flow and annulus losses optimisation, tip clearance losses optimisation). For example, the decrease of tip clearance relative value ($\Delta\bar{r} = \Delta r / h$) of all compressor blade rims by 1% causes the efficiency to increase by about 2%, whereas for turbines by 1.5 ÷ 2.5%.

The effect of particular methods of modelling real gas flow through an axial compressing stage on the stage efficiency is shown on the Fig. 2.

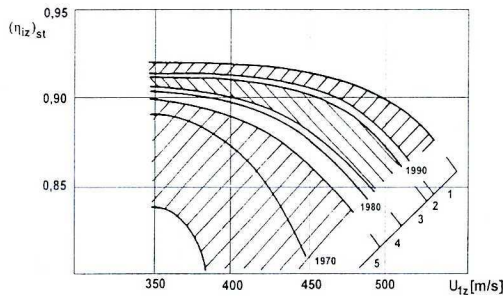


Fig. 2. Average values of isentropic efficiency of axial compressing stage versus peripheral speed at the entry external diameter of 1st stage rotor and type of motion equations describing the flow through blade rims: 1 – Navier-Stokes 3D, 2 – Navier-Stokes 2D, 3 – Euler 3D + BL (boundary layer), 4 – Euler 2D + BL, 5 – Potential flow [9]

The use of Navier-Stokes or Euler equations (2D or 3D) for quantitative flow analysis makes it possible to obtain the most accurate local processes representation in compressor and turbine rims, and adequate correction of their geometry ensures possible aerothermodynamical optimisation of stage rims [5], [6,]. Analogous notes concern another engine assemblies [5], [6], [7], [10], [11], [13].

3. Rerate with zero stage of compressor

In order to increase significantly the power (by about tens of percent) of a base turboprop or turboshaft engine (at slight increase of gas temperature before a gasifier turbine T_3^*) by increasing pressure ratio and mass flow rate of a compressor, an additional stage so-called „zero-stage” is added at the front of an existing compressor [3].

Proper selection of this zero-stage at the axial part of the main compressor of a turboprop or turboshaft engine with free power turbine requires keeping the geometry at the outlet of the zero-stage (4-4) and the inlet to the base engine main compressor (1-1), i.e., to fulfil the following requirements: $F_4 = F_1$, $\alpha_4 = \alpha_1$ and $M_4 = M_1$ or $\lambda_4 = \lambda_1$.

From the equation of continuity written for the flow between the main compressor inlet section (F_1) and zero-stage outlet section (F_4), results a direct relation determining the air mass flow rate in the main compressor with the zero-stage:

$$G_{10} = \frac{p_4^* s q(\lambda_4) \sin \alpha_4 \sqrt{T_1^*} F_4}{p_1^* s q(\lambda_1) \sin \alpha_1 \sqrt{T_4^*} F_1} G_1 \quad (4)$$

where, the pressure ratio of the zero-stage

$$\pi_{st0}^* = \frac{p_4^*}{p_1^*} \quad (5)$$

whereas the air stagnation temperature at the zero-stage outlet given by the following formula

$$T_{40}^* = T_1^* \left(1 + \frac{\pi_{st0}^* \frac{k-1}{k} - 1}{\eta_{st0}^*} \right) \quad (6)$$

then, the equation (4) may be written

$$G_{10} = \frac{G_1 \pi_{st0}^*}{\sqrt{1 + \frac{\pi_{st0}^* \frac{k-1}{k} - 1}{\eta_{st0}^*}}} \quad (7)$$

Table 2 presents the total pressure ratio π_{st}^* and stage polytropic efficiency η_p^* for different types of axial stages.

Table 2.

Average total pressure ratio and polytropic efficiency values obtained for one stage and different types of axial stages

Type of Stage	π_{st}^*	η_p^*
Subsonic	1.15 – 1.35	0.88 – 0.90
Transonic	1.4 – 1.8	0.85 – 0.88
Supersonic	≥ 1.9	0.81 – 0.85

The isentropic efficiency of the zero-stage may be determined from the relation:

$$\eta_{st0}^* = \frac{\pi_{st0}^* \frac{k-1}{k} - 1}{\pi_{st0}^* k \eta_p^* - 1} - \Delta\eta_{st0}^* \quad (8)$$

where: $\Delta\eta_{st0}^* = f(G_1)$ – correction for decrease of stage efficiency that takes into account the effect of radial clearance and boundary layer [2]. For example, when $G_1 \approx 5 \text{ kg/s}$ – $\Delta\eta_{st0}^* \approx 0.025$.

One selects of pressure ratio value considering the differences of polytropic efficiencies of axial compressing stages (Table 3). The air mass flow rate of the main compressor (modified) - G_1 and its pressure ratio π_C^* is determined from the compressor characteristic with the C-CT working line plotted. Earlier one shall find the value of nondimensional corrected rotational speed according to the relation:

$$n_{Ccor} = (n_{Ccor})_{dp} \sqrt{\frac{T_1^*}{T_{40}^*}} \quad (9)$$

where, for the main compressor of the PZL-10W engine $(n_{Ccor})_{dp} = 31\,486 \text{ rpm}$.

Total pressure ratio of the main compressor with a zero-stage of the modified engine is determined from the formula:

$$\pi_{C0}^* = \pi_C^* \cdot \pi_{st0}^* \quad (10)$$

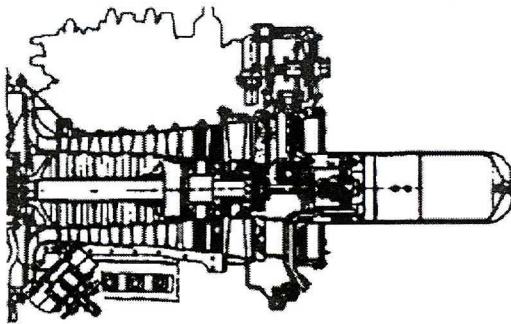


Fig. 3. The longitudinal section of compressor with zero-stage (darkened) of the modified PZL-10W engine of take-off power $N_{CT-O} = 888 \text{ kW}$ (1200 HP)

Exemplary results of calculations of selected performance of the turboshaft engine PZL-10W with compressor zero-stage are presented in Table 3.

Table 3.

Tabulation of take-off performance of the PZL-10W engine
with compressor zero-stage (S/L, static)

Parameter Name	Units	Designation	π_{st0}^*	
			1.275	1.30
Polytropic efficiency of zero-stage	–	$\eta_{p_{st0}}^*$	0.90	0.89
Isentropic efficiency of zero-stage	–	η_{st0}^*	0.871	0.86
Air stagnation temperature at outlet of zero-stage	K	T_4^*	311.93	314.23
Compressor corrected rotational speed	rpm	$n_{C_{cor}}$	30261	30151
Air mass flow rate of main compressor	kg/s	G_1	4.73	4.72
Pressure ratio of main compressor	–	π_C^*	7.70	7.66
Pressure ratio of main compressor with zero-stage	–	π_{C0}^*	9.817	9.959
Air mass flow rate of main compressor with zero-stage	kg/s	G_{10}	5.796	5.876
Engine shaft power with zero-stage of compressor	kW	N_{c0}	887.48	897.38
Specific fuel consumption of engine with zero-stage of compressor	kg/kWh	C_{c0}	0.3333	0.3325

4. Change of compressor pressure ratio

The problem of changing the compressor pressure ratio is most complex in the case of an axial-centrifugal compressor. For the axial-radial compressors of engines designed in the 1950s and 1960s, the number of axial stages was high ($N=5\div 7$) and was depended on the required pressure ratio of compressor and its partitioning between axial stages and the radial stage.

Large number of axial stages of these compressors resulted mostly from their limited load (pressure ratio). Besides, large number of axial stages of high efficiency influenced decisively the increase of the isentropic efficiency of axial-centrifugal compressor. Thanks to new technologies that utilise new materials, and owing to intensive development of CFD, it was possible to introduce modifications decreasing the number of axial stages ($N = 2\div 4$) and increasing the load (specific work and pressure ratio) of the radial part of axial-centrifugal compressor maintaining high value of its efficiency at the same time. Having determined the total pressure ratio of axial-centrifugal compressor – π_C^* , its isentropic efficiency – η_C^* and mass flow rate – G_{1cor} , one choses the number of axial stages – N . The geometry (diameters, stagger angles, etc.) and performance (loads, pressure ratios, efficiencies, etc.) of the stages are the same as the ones of the initial compressor stages of the base engine. Next, the method

of determining parameters of modified axial-centrifugal compressor can be illustrated with the following formulas [2]:

- Total pressure ratio of an axial part of compressor

$$\pi_{CA}^* = \prod_{i=1}^N \pi_{sti}^* \quad (11)$$

where: π_{sti}^* - total pressure ratio of the axial stage

- Total pressure ratio of a radial part of compressor

$$\pi_{CR}^* = \frac{\pi_C^*}{\pi_{CA}^*} \quad (12)$$

- Isentropic work of compression in the axial stage

$$(l_{is}^*)_{sti} = \frac{kR}{k-1} T_1^* \left(\pi_{sti}^{*\frac{k-1}{k}} - 1 \right) \quad (13)$$

- Effective work of compression in the axial stage

$$(l_{ef})_{sti} = \frac{(l_{is}^*)_{sti}}{\eta_{sti}^*} \quad (14)$$

where: η_{sti}^* - isentropic efficiency of the axial stage

- Design effective work of the axial stage

$$(l_e)_{sti} = \frac{(l_{ef})_{sti}}{K_{Hi}} \quad (15)$$

where: K_{Hi} - axial stage work factor

- Effective work of compression in the axial part of compressor

$$(l_{ef})_A = \sum_{i=1}^N (l_{ef})_{sti} \quad (16)$$

- Isentropic work of compression in the axial part of compressor

$$(l_{is}^*)_A = \frac{kR}{k-1} T_1^* \left(\pi_{CA}^{*\frac{k-1}{k}} - 1 \right) \quad (17)$$

- Isentropic efficiency of the axial part of compressor

$$\eta_{CA}^* = \frac{(l_{is}^*)_A}{(l_{ef})_A} \quad (18)$$

- Isentropic work of compression in the radial part of compressor

$$(l_{is}^*)_R = \frac{kR}{k-1} T_{2A}^* \left(\pi_{CR}^* \frac{k-1}{k} - 1 \right) \quad (19)$$

where: stagnation temperature at outlet of the axial part of compressor

$$T_{2A}^* = T_1^* \left(1 + \frac{\pi_{CA}^* \frac{k-1}{k} - 1}{\eta_{CA}^*} \right) \quad (20)$$

- Isentropic work of the axial-centrifugal compressor

$$(l_{is}^*)_C = \frac{kR}{k-1} T_1^* \left(\pi_C^* \frac{k-1}{k} - 1 \right) \quad (21)$$

- Effective work of compression in the axial-centrifugal compressor

$$(l_{ef})_C = \frac{(l_{is}^*)_C}{\eta_C^*} \quad (22)$$

- Effective work of the radial part of compressor

$$(l_{ef})_R = (l_{ef})_C - (l_{ef})_A \quad (23)$$

- Isentropic efficiency of the radial part of compressor

$$\eta_{CR}^* = \frac{(l_{is}^*)_R}{(l_{ef})_R} \quad (24)$$

- Design effective work of the radial part of compressor

$$l_{eR} = \frac{(l_{ef})_R}{K_{HR}} \quad (25)$$

where: K_{HR} – radial stage work done factor

- Impeller outer diameter

$$D_2 = \frac{60}{\pi n} \sqrt{\frac{l_{eR}}{(\mu + \alpha)}} \quad (26)$$

where: α - friction coefficient, μ - work coefficient

- The peripheral speed of impeller

$$U_2 = \frac{\pi D_2 n}{60} \quad (27)$$

where: n – rotational speed of the compressor shaft

or:

$$U_2 = \sqrt{\frac{(l_{ix}^*)_R}{\eta_h}} \quad (28)$$

Usually, hydraulic efficiency $\eta_h = 0,62 - 0,71$

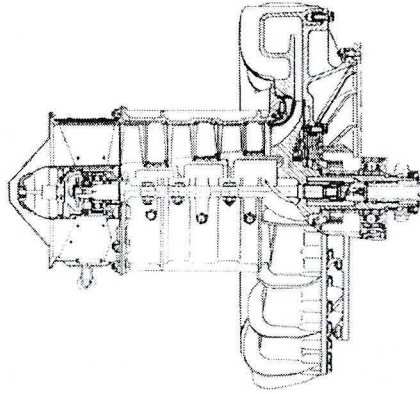


Fig. 4. The longitudinal section of a compressor of PZL-11 turboshaft engine

Figure 4 presents the section of compressor of the PZL-11 turboshaft engine with free power turbine whose selected parameters are given in Table 4.

Table 4.

GTD-350 base engine and PZL-11 modified engine data compressors

Parameter Name	Units	Designation	Engine Name	
			GTD-350	PZL-11
Isentropic efficiency of the axial – centrifugal compressor	–	η_C^*	0.775	0.81
Isentropic efficiency of the radial part of compressor	–	η_{CR}^*	0.738	0.807
Total pressure ratio of the axial – centrifugal compressor	–	π_C^*	6.16	6.26
Number of the axial stages	–	N	7	3
Total pressure ratio of the axial part of compressor	–	π_{CA}^*	3.403	1.673
Total pressure ratio of the radial part of compressor	–	π_{CR}^*	1.81	3.742
Impeller outer diameter	m	D_2	0.1849	0.211
Peripheral speed of the impeller at outlet	m/s	U_2	421.1	480.6

By reducing the number of the axial stages of the compressor of one base engine GTD-350 from 7 to 3 one could reduce the weight of the PZL-11 modified engine by about 3%. Somewhat smaller effect was obtained for the PZL-11A prototype engine made by WSK "PZL-Rzeszów" S.A. For this engine, the number of compressor axial stages was reduced to $N=4$.

5. Changes of rotational speeds of operational ratings

For turboprop and turboshaft engines, the principle of control at constant power turbine rotational speed is used regardless of engine loading and flight conditions. The change of performance versus gasifier shafting line speed (Fig. 5) arises as a result of increase or decrease of fuel mass flow rate supplied to the combustion chamber. At the same time, the speed governor of a power turbine (acting on a fuel-control system) or propeller governor (acting on propeller pitch) maintains constant power turbine speed.

Engine ratings (idle, T-O, OEI) differ in the values of compressor pressure ratio π_c^* , gas temperature before a gasifier turbine T_3^* , air mass flow rate through a compressor G , assembly efficiencies (η_i , σ_i), and gasifier shafting line speed n_{CT} . At constant geometry of ducts of engine assemblies, mutual dependence of basic parameters characterising operational ratings (power, fuel consumption) is determined by the steady-state operating line, C-CT (Equation 2). The main parameters characterising operational ratings of the engine are the following: gasifier shafting line speed n_{CT} , gas temperature before gasifier turbine T_3^* , or proportional to it, gas temperature before power turbine T_4^* . The gasifier shafting line speed determines the value of compressor pressure ratio π_c^* and air mass flow G while the gas temperature T_3^* (or T_4^*) effects considerably on performance at particular engine ratings. They also determine mechanical and thermal loading of assemblies. On the other hand, stresses at rotating parts are defined by the gasifier shafting line speed according to the relation:

$$\sigma_1 = \sigma_{dp} \frac{(n_{CT})_{dp1}^2}{(n_{CT})_{dp}^2} \quad (29)$$

where: σ_{dp} - stresses corresponding to design point speed $(n_{CT})_{dp}$.

The gas temperature T_3^* (and T_4^*) has a direct effect on strength of materials of turbine elements. Thus, safety factor for tensile stresses decreases with growth of shafting line speed, because:

$$K_{s1} = \frac{\sigma_{\tau 1}^T}{\sigma_1} \quad (30)$$

here: σ_{r1}^T - long-term strength, decreasing with growth of temperature of a part. Exemplary speed characteristics of the PZL-10W turboshaft engine are presented in Fig. 5.

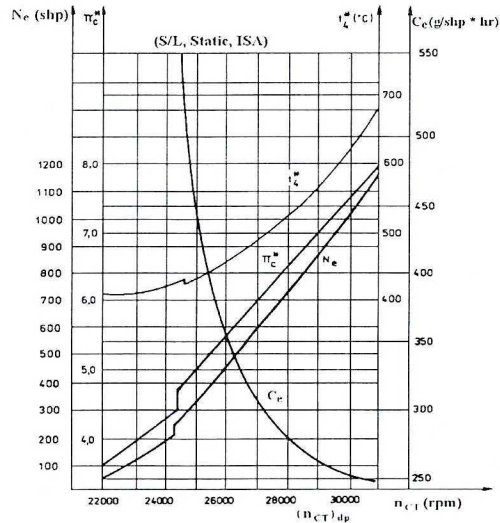


Fig. 5. Speed characteristics of the PZL-10W turboshaft engine

The increase of gasifier shafting line speed to the value of $(n_{CT})_{dp1} > (n_{CT})_{dp}$ involves an increase of pressure ratio, air mass flow through the compressor, and gas temperature before the turbine and as a consequence, the increase of engine power (uprated engine). On the other hand, the increase of n_{CT} speed causes the decrease of rotating assemblies efficiency because of increased flow velocities and usually, decreased safety margin of compressor (i.e., increased value of π_c^* / G_{1cor}). To ensure appropriate values of safety factors of rotating elements it is often necessary to change their materials. However, keeping recommended values of surge safety margin of compressor requires often to change the minimal section area of a nozzle or rotor rim of the gasifier and power turbine.

6. Change of gas temperature before turbine

It results from the analysis of turboshaft and turboprop engine performance that the output shaft power increases, and the specific fuel consumption decreases with the increase of gas temperature before gasifier turbine, T_3^* (and the associated temperature T_4^*) at given compressor pressure ratio. According to a detailed analysis of change of parameters of turboshaft engine with a free

power turbine presented in paper [4], when the value of shafting-line speed $n_{C_{cor}} = idem$ is kept constant, the gas temperature before gasifier turbine may be increased by the decrease of minimal section area of the nozzle rim of a power turbine or increased minimal section area of the nozzle rim of a gasifier turbine - Table 5.

Table 5.
Effect of minimal section area of a nozzle rim on chosen operating parameters
of a turboshaft engine

Minimal section area	Change direction	Parameter								
		T_3^*	T_4^*	π_{PT}^*	π_{CT}^*	$G_{1_{cor}}$	π_C^*	$\pi_C^* / G_{1_{cor}}$	N_{ePT}	C_c
$(F_{GV})_{PT}$	↑	↓	↓	↓	↑	↑ or idem	↓	↓	↓	↑
	↓	↑	↑	↑	↓	↓ or idem	↑	↑	↑	↓
$(F_{GV})_{CT}$	↑	↑	↑	↑	↓	↑ or idem	↓	↓	↑	↓
	↓	↓	↓	↓	↑	↓ or idem	↑	↑	↓	↑

To determine the degree of change of minimal section area of the nozzle rim of a power turbine $\Delta(F_{GV})_{PT}$ and minimal section area of the nozzle rim of a gasifier turbine $\Delta(F_{GV})_{CT}$, one takes advantage of the fact that for shafting-line speeds, at the design point of turboshaft and turboprop engines with free power turbine Laval numbers, $(\lambda_{GV})_{PT} > 0.9$ and $(\lambda_{GV})_{CT} > 0.9$. This makes it possible to use suitable flow similarity criterions for these rims [4].

Table 6 shows flow similarity criterions of nozzle rims of the PZL-10W turboshaft engine with free power turbine used for calculating, by two different methods, the changes of the stagnation gas temperature before a gasifier turbine at the constant value of a shafting-line speed $(n_{C_{cor}})_{dp} = idem$.

The Figure 6 presents shaft power ΔN_{ePT} values and gas stagnation temperature before a power turbine ΔT_4^* changes calculated and measured as a function of the nozzle rim minimal throat area of a compressor and power turbine. The calculations were done using the OST programme considering the flow similarity criterion of turbine nozzle rims specified in Table 6. The experimental works and calculations done by WSK "PZL-Rzeszów" S.A. fully proved the essential influence of $(F_{GV})_{PT}$ and $(F_{GV})_{CT}$ on the parameter and performance values of turboshaft engine with free power turbine.

Table 6.
Flow similarity criterions of turbine nozzle rims of the PZL-10W turboshaft engine

Criterion formula	Method of modification		Design point value	Unit
	$(F_{GV})_{PT} = idem$ $(F_{GV})_{CT} = var$	$(F_{GV})_{PT} = var$ $(F_{GV})_{CT} = idem$		
$\bar{A}_{PT} = \frac{(G_{GV})_{PT} \sqrt{T_4^*}}{(F_{GV})_{PT} p_4^*} = idem$	No	Yes	$3.826 \cdot 10^{-2}$	$\frac{kg \sqrt{K}}{s N}$
$A_{CT} = \frac{(G_{GV})_{CT} \sqrt{T_3^*}}{p_3^*} = idem$	No	Yes	$2.133 \cdot 10^{-4}$	$\frac{kg \sqrt{K}}{s Pa}$
$A_{PT} = \frac{(G_{GV})_{PT} \sqrt{T_4^*}}{p_4^*} = idem$	Yes	No	$5.931 \cdot 10^{-4}$	$\frac{kg \sqrt{K}}{s Pa}$
$\bar{A}_{CT} = \frac{(G_{GV})_{CT} \sqrt{T_3^*}}{(F_{GV})_{CT} p_3^*} = idem$	Yes	No	$2.601 \cdot 10^{-2}$	$\frac{kg \sqrt{K}}{s N}$

To the best of author's knowledge, the results presented in Fig. 6, are published for the first time.

7. MODELLING

The term modelling (i.e., designing with the use of flow similarity criteria) means to determining geometric, kinematic, and thermodynamic parameters of the so called model rotor machines (subscript M) that differ from real ones (subscript r) in dimensions, rotational speeds, pressures, temperatures, and mass flow rates at proper points of flow ducts but whose characteristics are identical (or similar). For adiabatic flow through engine compressor and turbine, for identical working medium whose properties, may be approximated as perfect gas properties, one may write the following similarity criteria [8], [15]:

– for a compressor

- mass flow parameter at the compressor entry

$$A_{Cr} = A_{CM} = \left(\frac{G_1 \sqrt{T_1^*}}{p_1^*} \right)_r = \left(\frac{G_1 \sqrt{T_1^*}}{p_1^*} \right)_M \quad (31)$$

- Laval number of tangential velocity at the rotor entry

$$\lambda_{u1r} = \lambda_{u1M} = \left(\frac{\pi D_C}{60 \sqrt{2} \frac{kR}{k+1}} \frac{(n_C)}{\sqrt{T_1^*}} \right)_r = \left(\frac{\pi D_C}{60 \sqrt{2} \frac{kR}{k+1}} \frac{(n_C)}{\sqrt{T_1^*}} \right)_M \quad (32)$$

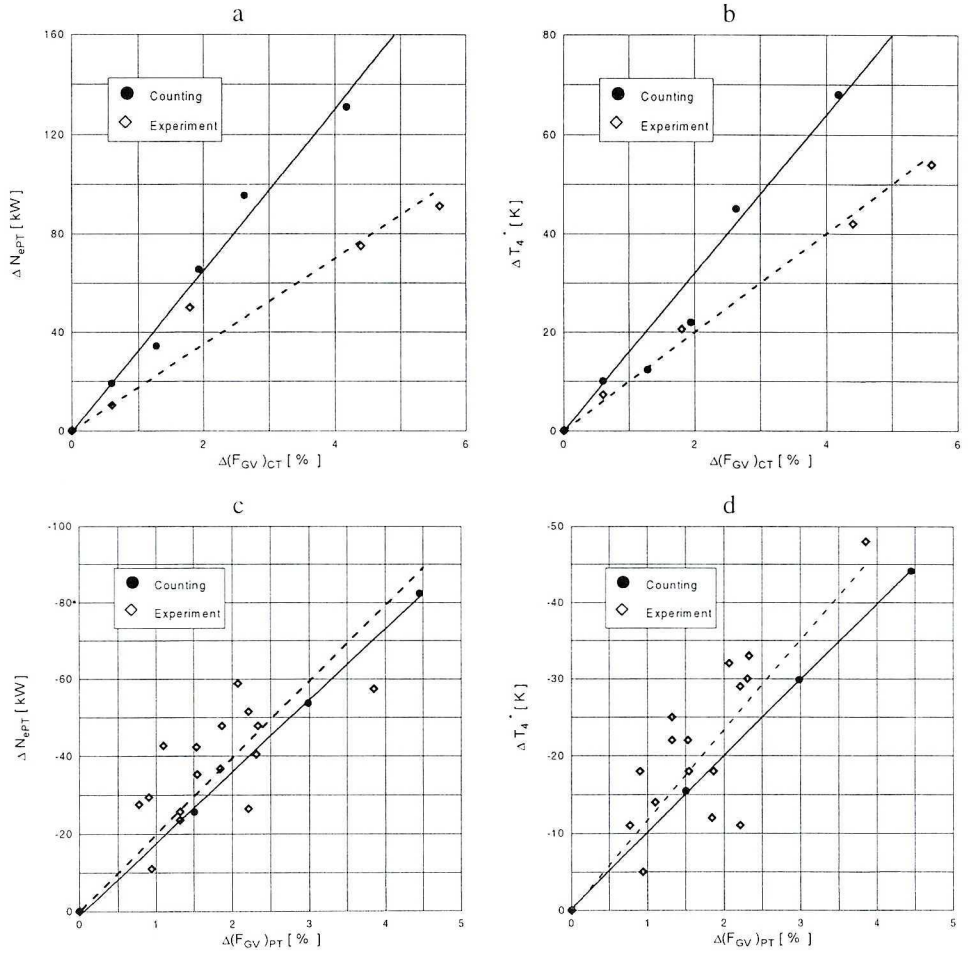


Fig. 6. The influence of increased minimal section area of nozzle rim of gasifier $\Delta(F_{GV})_{CT}$ and power $\Delta(F_{GV})_{PT}$ turbine on the change of gas temperature before power turbine ΔT_4^* and output shaft power ΔN_{ePT}

– for a turbine

- mass flow parameter at the turbine entry

$$A_{Tr} = A_{TM} = \left(\frac{G_3 \sqrt{T_3^*}}{p_3^*} \right)_R = \left(\frac{G_3 \sqrt{T_3^*}}{p_3^*} \right)_M \quad (33)$$

- Laval number of tangential velocity at the rotor entry

$$\lambda_{u1r} = \lambda_{u1M} = \left(\frac{\pi D_T}{60 \sqrt{2 \frac{k'R'}{k'+1}}} \frac{n_T}{\sqrt{T_3^*}} \right)_r = \left(\frac{\pi D_T}{60 \sqrt{2 \frac{k'R'}{k'+1}}} \frac{n_T}{\sqrt{T_3^*}} \right)_M \quad (34)$$

The compressor map of the base engine specified by the formula:

$$\begin{aligned} \pi_{Cr}^* &= f_1(q(\lambda_1), \lambda_{u1}) \\ \eta_{Cr}^* &= f_2(q(\lambda_1), \lambda_{u1}) \end{aligned}$$

may be used to choose parameters of a new compressor, i.e., the modelled one, that is geometrically similar to the base compressor. From the thermogasdynamical calculations of the engine modelled, one can determine total pressure ratio, π_{CM}^* , stagnation gas temperature before a turbine, T_{3M}^* , mass flow rate of air at the inlet, G_{IM} , assemblies efficiency, and total pressure and temperature of air at the inlet, T_{1M}^* , p_{1M}^* (determined by calculated flight conditions). Next, one may choose the design point of the modelled compressor of ordinate π_{CM}^* and abscissa $q(\lambda_1)$ providing suitable value of the surge margin of the compressor ΔK_C [4] on the compressor performance map of the real engine.

The inlet section area of the modelled compressor is determined from the continuity equation:

$$F_{C1M} = \frac{G_{IM} \sqrt{T_1^*}}{p_{1M}^* q(\lambda_1) s} \quad (35)$$

Where the constant:

$$s = \sqrt{\frac{k}{R}} \left(\frac{2}{k+1} \right)^{\frac{k+1}{2(k-1)}}$$

For the sake of geometrical similarity of the real and modelled compressors, the hub-tip diameter ratio at the compressor inlet equals: $\bar{d}_{C1M} = \bar{d}_{C1r}$, and the flow duct tip diameter of the modelled compressor is:

$$D_{C1M} = \sqrt{\frac{4 F_{C1M}}{\pi (1 - \bar{d}_{C1r})}} \quad (36)$$

From here, the scale factor, called the number of geometrical similarity, is given by equation:

$$\psi_C = \frac{D_{C_{IM}}}{D_{C_{Ir}}} = \sqrt{\frac{G_{IM}}{G_{Ir}}} \quad (37)$$

The relation (34) gives directly the equation:

$$(D_{C_i} n_C)_r = (D_{C_i} n_C)_M \quad (38)$$

from here:

$$n_{CM} = n_{Cr} \frac{D_{C_{Ir}}}{D_{C_{IM}}} = \frac{n_{Cr}}{\psi_I} \quad (39)$$

Similarly, one obtains the corrected rotational speed:

$$(n_{C_{cor}})_M = (n_{C_{cor}})_r \frac{1}{\psi_I} \quad (40)$$

The compressor map of the modelled compressor is found from the compressor map of the real compressor by replacing the values $(G_{1_{cor}})_r$ and $(n_{C_{cor}})_r$ by the values $(G_{1_{cor}})_M$ and $(n_{C_{cor}})_M$, where:

$$(G_{1_{cor}})_M = (G_{1_{cor}})_r \psi_I^2 \quad (41)$$

Table 7 shows selected parameters of modelled compressors, given in Fig. 7, calculated using the similarity criteria.

Table 7.

Principal parameters of the modelled compressors

Quantity and unit measure	Mass flow rate of air at compressor inlet G_1 [kg/s]		
	2.7	13.2	19.5
Scale – model coefficient	0.425	1.0	1.215
Corrected rotational speed [rpm]	45000	20350	16750
Outer diameter, rotor entrance [m]	0.1564	0.3458	0.4202
Inner diameter, rotor entrance [m]	0.0704	0.1556	0.1891

It should be noticed that the use of the criterion of flow dynamic similarity (analogous to the ones presented above and in Table 6) for a compressor and turbine makes it possible to model the geometry of gasifier shaf-line unit for engines of different performances and parameters – Fig. 7.

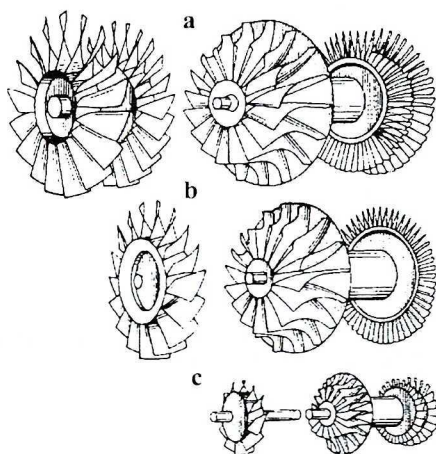


Fig. 7. Modelling of compressor and turbine shaft-lines of turboshaft engine for different scales
 [14] a - $\pi_c^* = 7.3$, $G_1 = 19.5$ kg/s; b - $\pi_c^* = 5.7$, $G_1 = 13.2$ kg/s; c - $\pi_c^* = 6.0$, $G_1 = 2.7$ kg/s

8. Final notes

The practise of developing modifications is a wide-spread approach in leading world-famous companies. Thus, each basic engine is manufactured along with a series of its modifications. For example, Turbomeca offers to its customers 15 modifications besides of the Arriel base turboshaft engine. The PT6A turboprop engine of Pratt & Whitney Canada has over 20 modifications with a wide range of performance.

Aerodynamic design capability has improved since the 1960s. Early designs were done using empirical rules and employed standard airfoil shapes [6], [7]. Blade-to-blade analysis was introduced in the 1970s, 3D Euler codes in the 1980s and 3D Navier-Stokes codes are in use today. Computational Fluid Dynamics (CFD) provides detailed flow pictures in turbomachines at lower cost than that of experimental investigations. Simultaneously, CFD facilitates quick and low-cost optimisation of the geometry of duct components of turbomachines. Considering the mentioned above, improvement of efficiency of engine units is a widely used method of modifying engines designed in the 1960s and 1970s. Similarly, the efficiency increase of the GTD-350 engine compressor made it possible to construct its modified version, GTD-350W whose take-off power has increased by over 15 kW.

The usage of subsonic zero-stage on the compressor of the TWD-10 turboprop engine ($N_{eT.O} = 706$ kW, $\pi_c^* = 7.4$, $G_1 = 4.58$ kg/s) changed the performance of the modified TWD-20 by tens of percent ($N_{eT.O} = 1066$ kW, $\pi_c^* = 9.55$, $G_1 = 5.9$ kg/s). If one needs a greater performance increase of the modified engine by applying this method, then the axial zero-stage should be a

transonic or supersonic one. Similarly, the application of a centrifugal zero-stage ensures strong performance increase [12]. The pressure ratio increase of an axial-centrifugal compressor associated with a reduction of the number of axial stages (from $N = 6$ to $N = 4$) was obtained by rerate the Allison Model 250 – C20B engine ($\pi_C^* = 7.0$). The modified axial-centrifugal compressor of the Model 250-C24 engine achieves a 3 percent increase in isentropic compressor efficiency and higher value of pressure ratio – $\pi_C^* = 8.0$. The shaft power and mass flow rate of air in the C24 engine are identical to these in the C20B. Specific fuel consumption is changed from 0.4 kg/kWh in the C20B to 0.358 kg/kWh in the C24. The increase of gasifier shaft-line speed by $\Delta n_{CT} = 600$ rpm makes it possible to obtain the modified PZL-10W1 engine of take-off power $N_{eT-O} = 700$ kW (Fig. 5) [1]. It should be noticed that the increase of operation ratings n_{CT} requires more comprehensive and expensive certification tests (than for modifications for which $n_{CT} = idem$). The modifications connected with changing gas temperature before the turbine, like: $(F_{GV})_{CT} = idem$, $(F_{GV})_{PT} = var$ or $(F_{GV})_{CT} = var$, $(F_{GV})_{PT} = idem$ when $n_{C\ cor} = idem$, causes the change of C-CT working line.

The superposition of both methods (Table 6) was used to obtain the modification designated as PZL-10W2, getting the power increase for particular operation ratings by about 100 kW [1]. For military versions of turboprop and turboshaft engines, we can observe a tendency of increasing the stagnation gas temperature before turbine being the result of designer's pursuit for reducing weight per horse-power even at the cost of shortening engine life.

From the point of view of performances of the turboshaft or turboprop engine, it is specially profitable to increase the compressor pressure ratio while increasing the turbine inlet temperature T_3^* .

Manuscript received by Editorial Board, May 29, 2000;
final version, September 07, 2000.

REFERENCES

- [1] Antas S., Kujda J.: Conceptual Design Study of PZL-10W engine with increased take-off power up to 1000 HP. WSK "PZL-Rzeszów" S.A., Doc. No. 19.0.470, 1997, pp. 101 (in Polish).
- [2] Antas S., Wolański P.: Thermogasdynamic Calculations of Aviation Turbine Engines. Publishing House of Warsaw University of Technology, Warsaw 1989, pp. 196 (In Polish).
- [3] Antas S. [et al]: Technical Analysis of Increasing the Power of the PZL-10W Turboshaft Engine by Using a Zero-Stage of a Compressor and Changing Operation Ratings. WSK "PZL-Rzeszów" S.A. Doc. No. 19.0.364, 1991, pp. 87 (in Polish).

- [4] Antas S.: The Selection of Turbine Critical Parameters for Providing Stable Compressor Operation Range. The Archive of Mechanical Engineering. Vol. XLVI, No 3, 1999, pp. 273÷299.
- [5] Antas S., Chmielniak T.: Stages of Realisation of Aviation Gas Turbine Engine. Calculations of Flow in Turbomachines. Transactions of the Institute of Aviation, z. 158, No. 3, 1999, pp. 75÷102 (in Polish).
- [6] Badger M [et al]: The PT6 Engine: 30 Years of Gas Turbine Technology Evolution. Transactions of the ASME. Journal of Engineering for Gas Turbines and Power. Vol. 116, April 1994, pp. 322÷330.
- [7] Byrd J.A.: A new Generation of Allison Model 250 Engines. Transactions of the ASME. Journal of Engineering for Gas Turbines and Power. Vol. 106, July 1984, pp. 703÷711.
- [8] Cholscevnikov K.V.: Theory and Calculations of Aircraft Turbo-machines. Mašinostroenie, Moscow, 1970 (in Russian).
- [9] Collective work: Aerodynamics - Direction Technique. SNECMA: Centre de Vilaroche. Division Recherches & Etudes Advances. Moissy-Cramayel, 1991.
- [10] Drake A.: Advancements in Process Market Compressors. Turbomachinery, z. 102, 1992, pp. 107÷120.
- [11] Karadimas G.: Propulsion System Design, Analysis and Integration with Airframe Using Advanced CFD Codes. Revue Scientifique SNECMA. No 4, June 1993, pp. 5÷15.
- [12] Lüdtke K.: Rerate of Centrifugal Compressors an Alternative for Production Increase and Efficiency Improvement. Turbomachinery, z. 108, 1995, pp. 239÷252.
- [13] McGuirk J.J., Palma J.M.L.M.: The Flow Inside a Model Gas Turbine Combustor: Calculations. Transactions of the ASME. Journal of Engineering for Gas Turbines and Power. Vol. 115, July 1993, pp. 594÷602.
- [14] Maslennikov M.M., Bethli J.G., Šalman J.I.: Turboshaft engines for helicopters, Mašinostroenie, Moscow, 1969 (in Russian).
- [15] Nečaev J.M., Fedorov R.M.: Theory of aircraft turbine engines. Vol. I, Mašinostroenie, Moscow, 1977 (in Russian).
- [16] Stevens E.C., Conn F.E.: Evolution of the Allison Model 250 Engine. SAE Transactions, Vol. 89, No. 800603, 1980.

Zagadnienia termogazodynamiczne metod modyfikacji konstrukcji silników śmigłowych i śmigłowcowych

Streszczenie

W artykule skrótkowo opisano przyczyny doskonalenia konstrukcji oraz przedstawiono aspekty termoaerodynamiczne metod tworzenia modyfikacji turbinowych silników śmigłowych i śmigłowcowych. Analiza teoretyczna metod modyfikacji dotyczy ogólnie zmian wydajności, przepływu oraz zakresu roboczego. Omówiono zatem kolejno następujące sposoby zmiany osiągnięć silnika: zmiana wartości współczynników jakości działania (sprawności) zespołów; wzrost sprężu i strumienia masy powietrza przepływającego przez sprężarkę poprzez zastosowanie stopnia zerowego; zmiana sprężu sprężarki przy zachowaniu strumienia masy powietrza przepływającego przez silnik; zmiana (tj. przesunięcie) przedziału prędkości obrotowych roboczych zakresów pracy; zmiana temperatury spiętrzenia spalin przed turbiną wytwornicową

przy utrzymaniu prędkości obrotowej pędni (zespołu wirnikowego wytwnicy) poprzez regulację pola powierzchni przekroju minimalnego wieńca dyszowego; modelowanie. Badania teoretyczne wpływu wymienionych metod modyfikacji na parametry użytkowe turbinowych silników śmigłowych i śmigłowcowych zilustrowano przykładami zastosowań.